Surface plasmon polariton enhanced by optical parametric amplification in nonlinear hybrid waveguide

F. F. Lu, T. Li,* J. Xu, Z. D. Xie, L. Li, S. N. Zhu, and Y. Y. Zhu

National Laboratory of Solid State Microstructures, College of Engineering and Applied Science, College of Physics, Nanjing University, Nanjing 210093, China

**taoli@nju.edu.cn*

Abstract: We theoretically studied nonlinear interactions between surface plasmon polariton (SPP) and conventional waveguide mode in nonlinear hybrid waveguide and proposed a possible method to enhance SPP wave via optical parametric amplification (OPA). The phase matching condition of this OPA process is fulfilled by carefully tailoring the dispersions of SPP and guided mode. The influences of incident intensity and phase of guided wave on the OPA process are comprehensively analyzed. It is found that not only a strong enhancement of SPP but also modulations on this enhancement can be achieved. This result indicates potential applications in nonlinear optical integration and modulations.

OCIS codes: (240.6680) Surface plasmons; (190.4410) Nonlinear optics, parametric processes; (230.7390) Waveguides, planar.

References and Links

1. J. J. Burke, G. I. Stegeman, and T. Tamir, "Surface-polariton-like waves guided by thin, lossy metal films," Phys. Rev. B Condens. Matter **33**(8), 5186–5201 (1986).
2. I. De Leon and P. Berini, "Theory of surface plasmon-polariton amplification in planar structures incorporating dipolar gain media," Phys. Rev. B **78**, 161401 (2008).
3. D. J. Bergman, and M. I. Stockman, "Surface plasmon amplification by stimulated emission of radiation: quantum generation of coherent surface plasmons in nanosystems," Phys. Rev. Lett. **90**(2), 027402 (2003).
4. R. F. Oulton, V. J. Sorger, T. Zentgraf, R. M. Ma, C. Gladden, L. Dai, G. Bartal, and X. Zhang, "Plasmon lasers at deep subwavelength scale," Nature **461**(7264), 629–632 (2009).
5. T. Holmgaard, and S. I. Bozhevolnyi, "Theoretical analysis of dielectric-loaded surface plasman-polariton waveguides," Phys. Rev. B **75**(24), 245405 (2007).
6. T. Holmgaard, J. Gosciniak, and S. I. Bozhevolnyi, "Long-range dielectric-loaded surface plasmon-polariton waveguides," Opt. Express **18**(22), 23009–23015 (2010).
7. R. W. Boyd, *Nonlinear Optics* (Elsevier Science, 2003).
8. R. A. Baumgartner, and R. Byer, "Optical parametric amplification," IEEE J. Quantum Electron. **15**(6), 432–444 (1979).
9. J. Armstrong, N. Bloembergen, J. Ducuing, and P. Pershan, "Interactions between light waves in a nonlinear dielectric," Phys. Rev. **127**(6), 1918–1939 (1962).
10. S. N. Zhu, Y. Y. Zhu, and N. B. Ming, "Quasi-phase-matched third-harmonic generation in a quasi-periodic optical superlattice," Science **278**(5339), 843–846 (1997).
11. H. J. Simon, D. E. Mitchell, and J. G. Watson, "Optical Second-Harmonic Generation with Surface Plasmons in Silver Films," Phys. Rev. Lett. **33**(26), 1531–1534 (1974).
12. H. J. Simon, R. E. Benner, and J. G. Rako, "Optical second harmonic generation with surface plasmons in piezoelectric crystals," Opt. Commun. **23**(2), 245–248 (1977).
13. S. Palomba, and L. Novotny, "Nonlinear excitation of surface plasmon polaritons by four-wave mixing," Phys. Rev. Lett. **101**(5), 056802 (2008).
14. P. B. Johnson, and R. W. Christy, "Optical constants of the noble metals," Phys. Rev. B **6**(12), 4370–4379 (1972).
15. G. Lifante, Integrated Photonics: Fundamentals (Wiley, England, 2003).
16. Z. Ruan, G. Veronis, K. L. Vodopyanov, M. M. Fejer, and S. Fan, "Enhancement of optics-to-THz conversion efficiency by metallic slot waveguides," Opt. Express **17**(16), 13502–13515 (2009).
17. R. H. Stolen, M. A. Bösch, and C. Lin, "Phase matching in birefringent fibers," Opt. Lett. **6**(5), 213–215 (1981).
18. T. Sugita, K. Mizuuchi, Y. Kitaoka, and K. Yamamoto, "31%-efficient blue second-harmonic generation in a periodically poled MgO:LiNbO3 waveguide by frequency doubling of an AlGaAs laser diode," Opt. Lett. **24**(22), 1590–1592 (1999).

#139447 - $15.00 USD Received 10 Dec 2010; revised 18 Jan 2011; accepted 21 Jan 2011; published 31 Jan 2011

19. H. Jiang, G. H. Li, and X. Y. Xu, "Highly efficient single-pass second harmonic generation in a periodically poled MgO:LiNbO3 waveguide pumped by a fiber laser at 1111.6 nm," Opt. Express **17**(18), 16073–16080 (2009).
20. Y. L. Lee, T. J. Eom, W. Shin, B.-A. Yu, D.-K. Ko, W.-K. Kim, and H.-Y. Lee, "Characteristics of a multi-mode interference device based on Ti:LiNbO3 channel waveguide," Opt. Express **17**(13), 10718–10724 (2009).
21. A. R. Davoyan, I. V. Shadrivov, and Y. S. Kivshar, "Quadratic phase matching in nonlinear plasmonic nanoscale waveguides," Opt. Express **17**(22), 20063–20068 (2009).
22. Z. J. Wu, X. K. Hu, Z. Y. Yu, W. Hu, F. Xu, and Y. Q. Lu, "Nonlinear plasmonic frequency conversion through quasiphase matching," Phys. Rev. B **82**(15), 155107 (2010).
23. G. J. Edwards, and M. Lawrence, "A temperature-dependent dispersion equation for congruently grown lithium niobate," Opt. Quantum Electron. **16**(4), 373–375 (1984).

1. Introduction

Surface Plasmon Polaritons (SPPs) are electromagnetic waves localized at the surface of a metal. Benefitting from its unique properties to squeeze electromagnetic energy into sub-wavelength scale, SPPs are better carriers of optical signal to be adopted in micro/nano-devices compared to conventional optical modes supported by dielectric waveguides. However, absorption caused by metal is one of the most frustrating problems, which greatly reduces its propagation length and limits its application. Up to now, several methods have been proposed to overcome the large losses of SPP. Long Range SPP [1] supported by dielectric/metal/dielectric structure once has been regarded as a promising mode with lower loss compared to conventional SPP, but it damages the strong localization of electromagnetic energy thus somewhat improper for miniaturization of photonic devices. Another widely studied method is using gain medium [2], a kind of optically active dielectric which can compensate the losses of SPP in propagation and even to achieve the Spaser [3,4]. Besides, hybrid waveguide, a combination of metal and dielectric media, provides a compromise between the field localization and low propagating loss in a more controllable manner, for example, the dielectric-loaded waveguide [5,6].

In this letter, we theoretically propose an alternative means to overcome the loss of SPP by producing amplification with the aid of auxiliary guided wave via nonlinear optical process. It is fulfilled in a hybrid waveguide, which is formed by nonlinear dielectric planar waveguide covered with a metallic layer so that it can be appropriately designed to support both the SPP and conventional guided modes. The coupling between SPP and guided modes tends to be possible since the field overlap is no too small, and the nonlinear optical process will be efficiently implemented. Thus conventional nonlinear optics effect [7–10] will be properly introduced to the plasmonic system. In fact, plasmonic nonlinear effects have arrested people's attention over a long period [11–13]. Our work will make an elaborate study of SPP involved optical parametric amplification in presence of a conventional guided mode as a pumping wave with doubled frequency in hybrid waveguide. The influences of the initial intensity and phase of these modes will be discussed in detail, which are considered to provide fruitful modulations on SPP amplification.

2. Theoretical model

Figure 1(a) schematically show the proposed hybrid planar waveguide, which is composed of a conventional dielectric waveguide (a high index medium NLD1 adjacent to a low index medium superstrate NLD2) and a metallic substrate. Without loss of generality, the dielectric function of metal is describe by the Drude model [14], and the nonlinear dielectric parts are defined by tensors in their dispersive permittivity. In this scheme, the metal substrate and NLD2 superstrate are both of semi-infinite thickness, and the middle waveguide layer (NLD1) is defined with thickness of *d*.

#139447 - $15.00 USD Received 10 Dec 2010; revised 18 Jan 2011; accepted 21 Jan 2011; published 31 Jan 2011

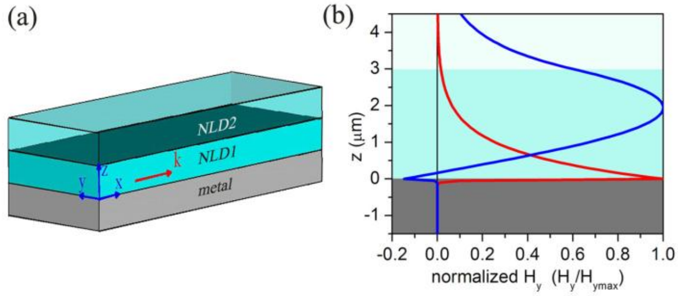

Fig. 1. (a) Schematic of a dielectric/dielectric/metal planar hybrid waveguide, where NLD1 and NLD2 represent the nonlinear dielectric with higher and lower refractive indices respectively; (b) The mode profiles of SPP (red) and TM_1 (blue) in hybrid waveguide, which are revealed as H_y.

Since SPP can be regarded as a kind of special waveguide mode, we use the method in Ref [15]. to derive the mode equations by adopting the appropriate boundary conditions as

$$k_1 d = n\pi + \tan^{-1}\left(f_1 \frac{p}{k_1}\right) + \tan^{-1}\left(f_2 \frac{q}{k_1}\right),\ n = 0,1,2... , \qquad (1)$$

where $k_1 = \sqrt{(k_0^2\varepsilon_{1z} - k^2)\varepsilon_{1x}/\varepsilon_{1z}}$, $p = \sqrt{k^2 - k_0^2\varepsilon_m}$ and $q = \sqrt{(k^2 - k_0^2\varepsilon_{2z})\varepsilon_{2x}/\varepsilon_{2z}}$, in which k is the in-plane wave vector (along x direction) of corresponding modes. The permittivity components ε_{1x}, ε_{1z}, ε_{2x}, ε_{2z} correspond to diagonal elements of permittivity tensor of NLD1 and NLD2. For TM polarization, $f_1 = \varepsilon_{1x}/\varepsilon_m$, $f_2 = \varepsilon_{1x}/\varepsilon_{2x}$; while for TE polarization, $f_1 = f_2 = 1$. By solving the dispersion relation of Eq. (1) with $n = 0$ in TM polarization case, we can find in-plane wave vector k always increases with the layer thickness d. As the condition $k > k_0(\varepsilon_{1z})^{1/2}$ is satisfied by increase d, k_1 turns to be imaginary indicating an exponentially decay field from the interface. Thus we can make sure that the expected SPP in hybrid planar waveguide is just TM_0 mode supported by this structure. Of course, a higher guided TM_1 mode (n = 1) will be accommodated by further increasing d to a proper value.

Afterwards, the nonlinear interaction of different electromagnetic modes has to be discussed to illustrate the optical parametric amplification (OPA) in hybrid waveguide. It is convenient to start from Maxwell equations

$$\begin{aligned} \nabla \times \vec{E}_i &= -\mu \frac{\partial \vec{H}_i}{\partial t}, \\ \nabla \times \vec{H}_i &= \varepsilon \frac{\partial \vec{E}_i}{\partial t} + \frac{\partial \vec{P}_i^{NL}}{\partial t}, \end{aligned} \qquad (2)$$

where ε and μ are the linear permittivity and permeability, and subscription i = 1,2 refers to the considered SPP and guided mode (TM_1) with frequencies of ω and 2ω, respectively. P^{NL} is the nonlinear polarization vector and $\partial P^{NL}/\partial t$ can be viewed as a source term that arises from the nonlinear interaction. For OPA process, a kind of second order nonlinear effect, we have $\vec{P}_1^{NL} = \varepsilon_0 \chi : \vec{E}_2^* \cdot \vec{E}_1$ and $\vec{P}_2^{NL} = (1/2)\varepsilon_0 \chi : \vec{E}_1 \cdot \vec{E}_1$. Tensor χ is the second order nonlinear susceptibility. According to coupled mode theory in waveguide, E_i and H_i can be expanded in terms of all canonical modes at the same frequency [15]: $E_l = \sum A_l(x) E_l(z)\exp(ik_l x)$, $H_l = \sum A_l(x) H_l(z)\exp(ik_l x)$. The waves are assumed to propagate along + x direction; $A_l(x)$ is the amplitude, which evolves with x due to coupling between different modes and propagation loss; $E_l(z)$ and $H_l(z)$ are mode profiles which have been

#139447 - $15.00 USD Received 10 Dec 2010; revised 18 Jan 2011; accepted 21 Jan 2011; published 31 Jan 2011

normalized as $\frac{1}{2}\int_{-\infty}^{+\infty}\vec{e}_x \cdot \mathrm{Re}\left\{\vec{E}_l(z)\times\vec{H}_l^*(z)\right\}dz = 1$. Following the method from Ref [16], the coupling between SPP and a guided mode in hybrid waveguide can be described by coupled wave equations:

$$\begin{aligned}\frac{\partial A_1}{\partial x} &= -\frac{\alpha_1}{2}A_1 + i\frac{\omega\varepsilon_0}{4}\kappa_1 A_1^* A_2 e^{i(\beta_2-2\beta_1)x},\\ \frac{\partial A_2}{\partial x} &= -\frac{\alpha_2}{2}A_2 + i\frac{\omega\varepsilon_0}{4}\kappa_2 A_1^2 e^{-i(\beta_2-2\beta_1)x},\end{aligned} \tag{3}$$

where β_i and $\alpha_i/2$ (i = 1,2) are real part and imaginary part of corresponding wave vectors, i.e., $k_i = \beta_i + \mathrm{i}\alpha_i/2$; α_i is defined as absorption coefficient; and κ_i is the coupling coefficient that defined as $\kappa_1 = \int \chi : \vec{E}_2\vec{E}_1^* \cdot \vec{E}_1^* dz$, $\kappa_2 = \int \chi : \vec{E}_1\vec{E}_1 \cdot \vec{E}_2^* dz$. The first term at right side for both equations corresponds to an attenuation indicating the energy conversions between different modes have to overcome losses proportional to absorption coefficient. Thus the power of SPP will not be amplified until the gains from the other electromagnetic mode obviously surpass the losses of SPP. Besides, the phase condition, $\Delta\beta = \beta_2 - 2\beta_1$, also directly affects the conversion efficiency. Due to the dispersion caused by nonlinear material, it is usually difficult to satisfy phase matching conditions. Phase mismatching ($\Delta\beta \neq 0$) will lead to cycle flows of energy between these two modes and limit the one-way conversion efficiency, making the amplification of SPP impossible.

In fact, the phase mismatch from the medium dispersion is a common problem in the nonlinear optical parametric process. During the past few decades, several methods have been developed to solve this problem (e.g., birefringence phase matching (BPM) [17] and quasi phase matching (QPM) [9,10]). However, most of these works were carried out in crystal optics regime without emphasizing the spatial confinement. To achieve an efficient optical parametric process in a waveguide or plasmonic system still remain considerable difficulties [18–21]. More recently, the QPM technique was theoretically proposed to realize the plasmonic frequency conversion by adopting the periodically poled nonlinear crystal as the dielectric environment [22], but it consequently increases the complexity in structure fabrications. Fortunately, the SPP wave itself has a larger wave vector compared with the light and guided wave in adjacent medium. According to Eq. (3), by defining $\beta_1(\omega)$ and $\beta_2(2\omega)$ as the wave vectors of SPP and guided mode respectively, the phase matching condition $2\beta(\omega) = \beta(2\omega)$ will be appropriately obtained by carefully adjusting the modes dispersions. In this regard, it is reasonable to using a guided wave of $\beta_2(2\omega)$ as an auxiliary light to compensate the propagating loss of SPP and even amplify it.

3. Example and analysis

To be specific, we consider silver for the metal substrate and $LiNbO_3$ for the anisotropic nonlinear dielectric that forms a conventional dielectric planar waveguide [20]. For simplification, the dielectric constant of the high index layer (middle LND1 layer) is simply defined by $\varepsilon_{1i} = \varepsilon_{2i} + 0.04$ ($i = x,y,z$), corresponding to a numerical aperture of about 0.2 for the conventional dielectric waveguide, where ε_{2i} is permittivity tensor elements of common $LiNbO_3$ [23]. To obtain high conversion efficiency and satisfactory amplification, it is best to make use of the largest component of nonlinear coefficient of χ, d_{33} for $LiNbO_3$ [23]. Thus it is preferable to orientate the crystalline axis along direction z, and use TM_1 mode as the auxiliary pumping wave, the coupling coefficients can be simplified by only considering the transverse fields as

$$\kappa_1 = \int d_{33}E_{2,z}(E_{1,z}^*)^2 dz = \kappa^*,\ \ \kappa_2 = \int d_{33}E_{2,z}^*(E_{1,z})^2 dz = \kappa, \tag{4}$$

since the integration over the longitudinal components (d_{31}, d_{22} and $E_{i,x}$) is too small and can be neglected as well as Ref. 20. The thickness of the middle layer (NLD1) is set to be 3μm. To

#139447 - $15.00 USD Received 10 Dec 2010; revised 18 Jan 2011; accepted 21 Jan 2011; published 31 Jan 2011

obtain phase matching, the wavelength of SPP and TM_1 mode is selected carefully. Dispersion relations of SPP and TM_1 mode are plotted in Fig. 2(a). Since phase matching condition can also be described as $n_{TM1} = n_{SPP}$, we plot frequency versus effective index in the inset of Fig. 2(a) to make it more obvious. The intersection point of the two curves, 168.4THz for SPP and 336.8THz for TM_1, indicates the satisfaction of phase matching. The corresponding effective indices are $n_{SPP} = 2.1731 + i0.001$ and $n_{TM1} = 2.1731 + i2.593 \times 10^{-6}$. Figure 1(b) shows the mode profiles of SPP and TM_1 used in this work. The field of SPP is tightly localized at the metal surface, with over 93% power confined in a 1μm thin dielectric layer, while only ~90% power of the TM_1 mode in the 3μm waveguide layer though it has a doubled frequency. The priority of SPP as the sub-wavelength waveguide is clearly demonstrated.

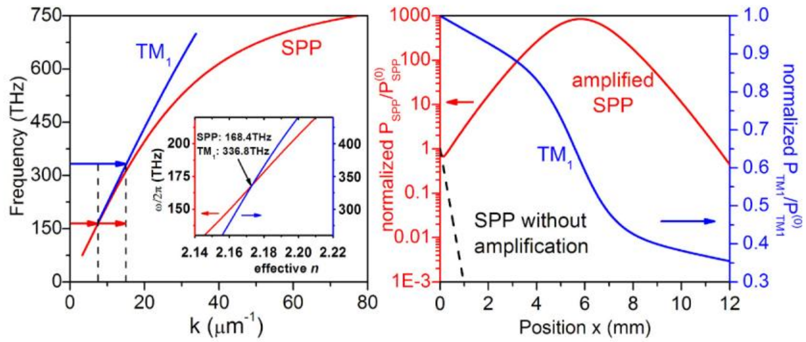

Fig. 2. (a) Dispersion relations of SPP (red curve) and TM_1 mode (blue curve) in hybrid waveguide. Inset shows the frequency vs. effective index. (b) Evolutions of normalized intensity of SPP (left logarithm scale) and TM_1 (right linear scale) modes in propagations, where the incident initial intensities are defined as $P_{SPP}^{(0)} = 1$kW/cm and $P_{TM1}^{(0)} = 50$MW/cm. A decay tendency of a pure SPP without amplification is also depicted as the dashed line.

Figure 2(b) shows the result of SPP amplification by OPA process by solving Eq. (3) with the simplified coupling coefficient [Eq. (4)], where the solid curves show the evolutions of power amplification of SPP (red curve in logarithm scale) and the pumped TM_1 power (blue in linear scale). The calculation is performed with incident intensity of 1kW/cm for SPP mode as a seed signal and 50MW/cm and for TM_1 guided mode as the pumping wave. The highest conversion efficiency is 1.69% and the peak of SPP appears at the position of 5.8 mm. To make a comparison, we also plot the trend of SPP attenuation without the TM_1 pumping wave (the dashed curve). It is clearly found that the intensity of this pure SPP drops to 1/*e* after only about 140μm, while SPP interacted with pumping wave gets amplification by about 845 times at the peak position.

Owing to the nature of second order nonlinear effect, this SPP OPA process should depend on the intensity of incident pumping TM_1 mode. In Fig. 3(a), OPA efficiency (left label) and the SPP amplification peak position (right label) with respect to the pumping intensity are depicted. It is apparently shown that the OPA process has a threshold pumping power ($P_{TM1}^{(0)}$~35MW/cm), below which the pumping TM_1 is unable to amplify the seed SPP and no SPP peak in propagation can be observed as a result. When the pumping intensity exceed the threshold, the efficiency increases rapidly (from 0% to 27% as $P_{TM1}^{(0)}$ ranges from 35 to 150MW/cm), while the SPP peak position experiences a maximum value (at $P_{TM1}^{(0)}$~43MW/cm) and tends to descend with the increase of $P_{TM1}^{(0)}$. In addition, we plot another OPA dependence of the intensity of seed SPP for a comparison as shown in Fig. 3(b), where the intensity of seed SPP ranges from 0.1kW/cm to 10kW/cm while the efficiency varies within a narrow range (1% ~2.5%). This influence of the amplification effect is rather weaker than $P_{TM1}^{(0)}$. This phenomenon is reasonably explained by deducing coupled wave equation from Eq. (3) to

#139447 - $15.00 USD Received 10 Dec 2010; revised 18 Jan 2011; accepted 21 Jan 2011; published 31 Jan 2011

$$\frac{d|A_1|}{dx} = \frac{1}{2}|A_1|[-\alpha_1 + \frac{1}{2}\omega\varepsilon_0|\kappa||A_2|\sin\psi(x)], \tag{5a}$$

$$\frac{d|A_2|}{dx} = \frac{1}{2}|A_2|[-\alpha_2 - \frac{1}{2}\omega\varepsilon_0|\kappa|\frac{|A_1|^2}{|A_2|}\sin\psi(x)], \tag{5b}$$

where $\psi(x) = \Phi + 2\varphi_1(x)\text{-}\varphi_2(x)$, $A_1 = |A_1|\exp[i\varphi_1(x)]$, $A_2 = |A_2|\exp[i\varphi_2(x)]$ and $\kappa = |\kappa|\exp(i\Phi)$. To get an amplification of SPP, $d|A_1|/dx>0$ should be satisfied. But the absorption coefficient (α_1) of SPP, obviously acts as the obstacle for the energy transfer from TM_1 to SPP. Then, we can get a critical intensity of TM_1 by solving $d|A_1|/dx = 0$, and obtain $|A_2| = 2\alpha_1[\omega\varepsilon_0|\kappa|\sin\psi(x)]^{-1}$, which corresponds to a balance value for a "lossless" SPP. On one hand, this critical balance value of P_{TM1} determines the threshold of $P_{TM1}^{(0)}$; on the other hand, it results in an SPP peak in propagation [see Fig. 2(b)]. In the peak position, the pumping energy decreases to the balance value, after which the pumping gain is overcome by the loss and leads to attenuation of SPP wave. Commonly, with stronger incident intensity SPP signal will be amplified at a shorter distanced due to the higher enhancement rate indicated in Eq. (5)a), which coincides with the major tendency. However, if the pumping intensity is merely above the threshold, the amplification will stop soon since the energy may consume to below the balance value quickly within a short distance. With the pumping energy increases, this distance will extend and a maximum peak position emerges at a proper value of $P_{TM1}^{(0)}$. It well explains the non-monotonous evolution of the SPP peak position in Fig. 3(a). Besides, Eq. (5)a) and (5b) also indicate the OPA efficiency is more relevant to $|A_2|$ than $|A_1|$ revealing different dependences on the intensity of pumping TM_1 and seed SPP in Fig. 3(a) and 3(b), respectively.

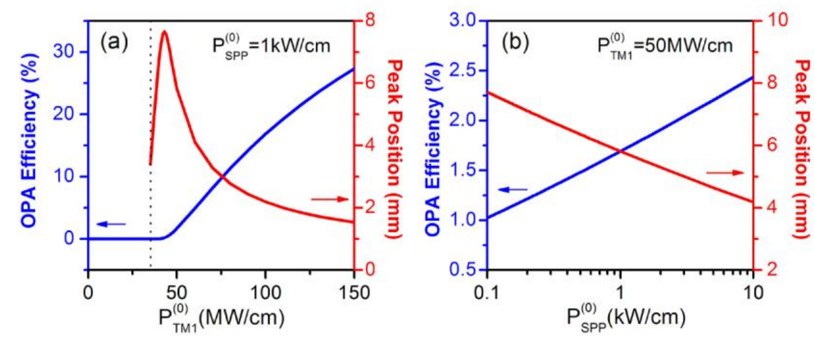

Fig. 3. (a) OPA efficiency and SPP peak position as a function of the incident intensity of TM_1; (b) OPA efficiency and SPP peak position as a function of the incident intensity of seed SPP.

#139447 - $15.00 USD Received 10 Dec 2010; revised 18 Jan 2011; accepted 21 Jan 2011; published 31 Jan 2011

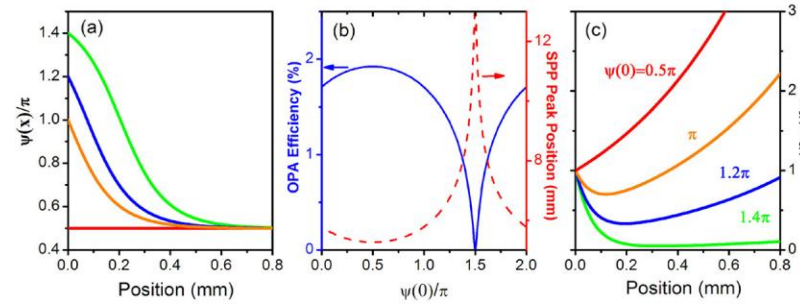

Fig. 4. (a) Phase evolutions with different incident phases, where $\psi(x) = \Phi + 2\varphi_1(x)$-$\varphi_2(x)$; (b) OPA efficiency and SPP peak position as the functions of incident phase $\psi(0)$, where $P_{TM1}^{(0)}$ = 50MW/cm and $P_{SPP}^{(0)}$ = 1kW/cm; (c) Evolutions of SPP intensity as propagation in condition of different incident pumping phases.

Another aspect should be addressed is the incident phase of SPP and TM_1 mode, which were both set to zero in previous calculations, i.e., $\varphi_1(0) = \varphi_2(0) = 0$. In fact, this phase is another important factor that affects the optical parametric process, according to Eq. (5)a) and (5b). We can derive the changes of phase from coupled wave equations as

$$\frac{d\varphi_1}{dx} = \frac{1}{4}\omega\varepsilon_0 |\kappa||A_2|\cos\psi(x), \tag{6a}$$

$$\frac{d\varphi_2}{dx} = \frac{1}{4}\omega\varepsilon_0 |\kappa|\frac{|A_1|^2}{|A_2|}\cos\psi(x). \tag{6b}$$

Though phase matching condition is satisfied between the two different modes, the phase still changes with propagating until a stable value is obtained (ψ = 0.5π), which is clearly revealed in the evolutions of the phases with different initial value (0.5π, 1.0π, 1.2π and 1.4π) in Fig. 4(a). According to Eq. (6)a) and (6b), $\cos\psi(x) = 0$ [or $\psi(x) = (1/2 + n)\pi$] is stable values for the phase. However, for even and odd number n, $\sin\psi(x)$ is 1 and −1 respectively, which directly decides the sign of $d|A_1|/dx$ according to Eq. (5)a). Thus, for some improper incident phases, OPA efficiency may be much lower and even get a negative contribution at the beginning. In this case, the SPP wave has to propagate much longer and experience extra losses until the phases get a stable value beneficial to SPP amplification. To prove our prediction, we change $\psi(0)$ from 0 to 2π to see the influence of incident phase. Figure 4(b) shows the OPA efficiency and peak position of different $\psi(0)$, where the incident intensities of TM_1 and SPP are 50MW/cm and 1kW/cm respectively. When $\psi(0)$ = 1.5π (corresponding to $\sin\psi(0) = -1$), a dip of efficiency appears together with a longest SPP peak position as predicted, while the highest efficiency is achieved at $\psi(0)$ = 0.5π. In Fig. 4(c), the intensity evolution of SPP with respect to different initial phase $\psi(0)$ are shown in different color curves, respectively. Combined with the phase evolution [Fig. 4(a)], we may find when incident phase at desirable value, such as 0.5π, ψ(x) reach the stable value immediately and SPP get amplified once the process started. For some improper incident phases near to undesirable value, for example, $\psi(0)$ = 1.4π, a long distance of propagation is necessary to get a desirable stable phase value for amplification of the seed SPP wave. For such incident phases indeed, SPP will firstly decay to an extremely low level before getting amplified.

4. Discussions

According to above results and analyses, we prove the possibility of obtaining enhanced SPP by optical parametric amplification in this nonlinear hybrid waveguide. In principle, this phenomenon arises from the interaction of two optical modes via the nonlinear effect. For more general consideration, such energy exchanges may exist in more cases, for example,

#139447 - $15.00 USD Received 10 Dec 2010; revised 18 Jan 2011; accepted 21 Jan 2011; published 31 Jan 2011

other higher ordered guided modes. However, different from the small field overlap of those higher ordered modes that commonly leads to low conversion efficiency, the field overlap of SPP and TM_1 mode is acceptable [see Fig. 1(b)], which fortunately provides us the possibility to realize the direct phase matching condition without any additional structural design (like Ref. 22). In fact, other second order nonlinear effects between SPP and conventional waveguide mode also can be derived in such kind of nonlinear hybrid waveguide. For example, the reversed process of this OPA, i.e., second harmonic generation from the SPP to the double-frequency waveguide mode, is reasonably expected as long as the phase matching condition is satisfied. Therefore, this scheme provides a new way not only to achieve the frequency conversions but also to realize the switches between the conventional guide wave and subwavelength SPP wave. From this point of view, such a hybrid waveguide also can be regarded as a coupler from radiative light to evanescent wave and vice versa.

Nevertheless, the revealed SPP amplification is still an important application of this nonlinear optical process. It may really provide opportunities to overcome the propagating loss of SPP rather than using a common gain medium. Furthermore, from our detailed analyses of the OPA influenced by the pumping intensity and phase tuning, this method reveals convenient modulations on the SPP wave at will, but not a merely amplification. In this sense, information can be loaded on the pumping guided wave to control SPP behavior, which is considered very important in future subwavelength integration and modulations.

5. Conclusion

In summary, a new method is proposed to realize an optical parametric amplification for an SPP wave in nonlinear hybrid waveguide. Taking advantage of the different dispersion of SPP mode and conventional guided wave, we desirably obtain the phase matching condition between these two modes, which is of vital importance for the nonlinear optical parametric process. Our results definitely indicate that with the aid of auxiliary pumping wave (TM_1 mode) the SPP wave can be loss-compensated and even amplified to a high level as the pumping energy is large enough. It surely suggests possible applications as subwavelength waveguide that overcome the usual propagating loss. According to our detailed investigations, the OPA efficiency and process are found closely related with intensity of the pumping guided wave and its initial phase with respect to that of SPP. This phase tuning notably provides a tunable modulation method potentially in the future subwavelength optical integrations.

Acknowledgement

The authors thank Dr. X. P. Hu for beneficial discussions. This work is supported by the State Key Program for Basic Research of China (Nos. 2010CB630703, 2009CB930501), the National Natural Science Foundation of China (Nos. 10974090, 60990320 and 11021403), and the National Undergraduates Innovation Program of China.

#139447 - $15.00 USD Received 10 Dec 2010; revised 18 Jan 2011; accepted 21 Jan 2011; published 31 Jan 2011